Determination of the C4–H Bond Dissociation Energies of NADH Models and Their Radical Cations in Acetonitrile

Xiao-Qing Zhu,* Hai-Rong Li, Qian Li, Teng Ai, Jin-Yong Lu, Yuan Yang, and Jin-Pei Cheng*[a]

Abstract: Heterolytic and homolytic bond dissociation energies of the C4–H bonds in ten NADH models (seven 1,4-dihydronicotinamide derivatives, two Hantzsch 1,4-dihydropyridine derivatives, and 9,10-dihydroacridine) and their radical cations in acetonitrile were evaluated by titration calorimetry and electrochemistry, according to the four thermodynamic cycles constructed from the reactions of the NADH models with *N*,*N*,*N*′,*N*′-tetramethyl-*p*-phenylenediamine radical cation perchlorate in acetonitrile (note: C9–H bond rather than C4–H bond for 9,10-dihydroacridine; however, unless specified, the C9–H bond will be described as a C4–H bond for convenience). The results show that the energetic scales of the heterolytic and homolytic bond dissociation energies of the C4–H bonds cover ranges of 64.2 – 81.1 and 67.9 – 73.7 kcal mol^{-1} for the neutral NADH models, respectively, and the energetic scales of the heterolytic and homolytic bond dissociation energies of the $(C4–H)^{\bullet+}$ bonds cover ranges of 4.1 – 9.7 and 31.4 – 43.5 kcal mol^{-1} for the radical cations of the NADH models, respectively. Detailed comparison of the two sets of C4–H bond dissociation energies in 1-benzyl-1,4-dihydronicotinamide (BNAH), Hantzsch 1,4-dihydropyridine (HEH), and 9,10-dihydroacridine ($AcrH_2$) (as the three most typical NADH models) shows that for BNAH and $AcrH_2$, the heterolytic C4–H bond dissociation energies are smaller (by 3.62 kcal mol^{-1}) and larger (by 7.4 kcal mol^{-1}), respectively, than the corresponding homolytic C4–H bond dissociation energy. However, for HEH, the heterolytic C4–H bond dissociation energy (69.3 kcal mol^{-1}) is very close to the corresponding homolytic C4–H bond dissociation energy (69.4 kcal mol^{-1}). These results suggests that the hydride is released more easily than the corresponding hydrogen atom from BNAH and vice versa for $AcrH_2$, and that there are two almost equal possibilities for the hydride and the hydrogen atom transfers from HEH. Examination of the two sets of the $(C4–H)^{\bullet+}$ bond dissociation energies shows that the homolytic $(C4–H)^{\bullet+}$ bond dissociation energies are much larger than the corresponding heterolytic $(C4–H)^{\bullet+}$ bond dissociation energies for the ten NADH models by 23.3 – 34.4 kcal mol^{-1}; this suggests that if the hydride transfer from the NADH models is initiated by a one-electron transfer, the proton transfer should be more likely to take place than the corresponding hydrogen atom transfer in the second step. In addition, some elusive structural information about the reaction intermediates of the NADH models was obtained by using Hammett-type linear free-energy analysis.

Keywords: bond energy · calorimetry · effective charge · NADH models · radical ions

Introduction

The reduced form of the nicotinamide adenine dinucleotide coenzyme (NADH) plays an important role in many bioreductions by transferring a hydride ion or electron to the surrounding substrates [Eq. (1)].[1] The mechanistic details of the hydride transfer has been a subject of great interest and is increasingly drawing the attention of researchers.[2, 3] One of the issues in focus is whether the hydride transfer proceeds by direct one-step or multistep sequence: electron/proton/electron, electron/hydrogen atom, or hydrogen atom/electron (Scheme 1). Based on published experimental results, a direct one-step mecha-

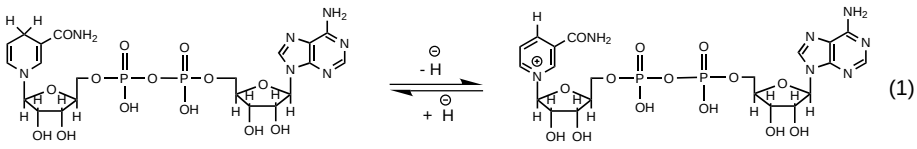

NADH NAD$^+$ (1)

[a] Prof. X.-Q. Zhu, Prof. J.-P. Cheng, H.-R. Li, Dr. Q. Li, T. Ai, J.-Y. Lu, Y. Yang
Department of Chemistry
State Key Laboratory of Elemento-Organic Chemistry
Nankai University, Tianjin 300071 (China)
Fax: (+86) 022-2350-2458
E-mail: xqzhu@nankai.edu.cn

  0947-6539/03/0904-0871 $ 20.00+.50/0

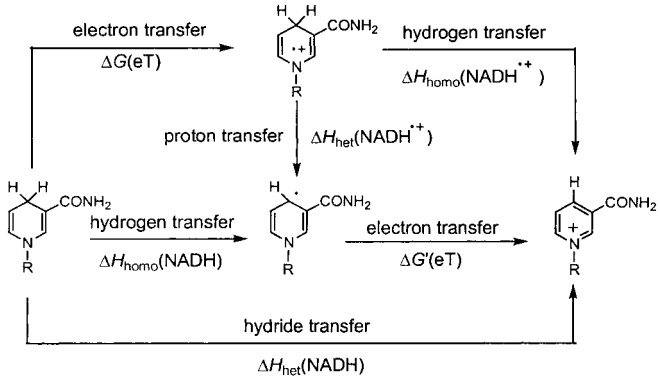

Scheme 1. Possible pathways of the hydride transfer from NADH.

nism was suggested for the reductions of ketones, aldehydes, imines, etc.[4] However, at the same time, a multi-step sequence mechanism was also proposed for the reductions of Fe^{III}, Fc^{+}, and many other single-electron oxidants.[5] Moreover, much conflicting evidence can be found for the same NADH mimic reaction, such as the reduction of quinone derivatives.[6] In short, the mechanistic details of the hydride transfer is still unclear at present; no common view yet explains all the diverse and confusing experimental results. Clearly, a detailed thermodynamic analysis on each mechanism-step for the hydride transfer from NADH and its models must be performed to completely solve this important problem.[7]

Examination of past reports on this subject shows that although there are some chemists, such as Saveant and coworkers,[8] who devoted much time to the study of the thermodynamics of NADH and its models, their main attention was limited to the electrochemistry and acid-base equilibria of NADH/NAD^{+} analogues. Rather scant attention has been paid to the detailed thermodynamic analysis on each mechanistic step for the hydride transfer from NADH and its models. From Scheme 1, it is clear that lack of knowledge about the energies of the related bond dissociation of NADH and its models prevents us making a detailed thermodynamic analysis on each mechanistic step for the hydride transfer. However, despite the clear importance and necessity of the bond energy data of NADH and its model compounds, essentially no direct determination of the C4–H bond dissociation energies either for the neutral NADH models or for their corresponding radical cations have yet been reported, except for some relative dissociation energies of the C4–H bond for a few NADH models[9] and estimation for the absolute dissociation energy of the C4–H bond for only a limited few NADH models.[10] To access the thermodynamic data of each mechanistic step for the hydride transfer from NADH and its models, as shown in Scheme 1, the key work is to determine the heterolytic and homolytic C4–H bond dissociation energies in NADH and its radical cation $NADH^{\bullet+}$ [Eqs. (2)–(5)]. Since it is impossible to obtain them directly by using the well-known thermodynamic approaches introduced by Bordwell,[11] Arnett,[12] and others,[13] it is necessary to develop a new method suitable for the determination of the C4–H bond scission energies in solution; this has been a goal in our research program for a long time. Recently,

$$NADH \rightarrow NAD^{+} + H^{-} \qquad \Delta H_{het}(NADH) = ? \qquad (2)$$

$$NADH \rightarrow NAD^{\bullet} + H^{\bullet} \qquad \Delta H_{homo}(NADH) = ? \qquad (3)$$

$$NADH^{\bullet+} \rightarrow NAD^{\bullet} + H^{+} \qquad \Delta H_{het}(NADH^{\bullet+}) = ? \qquad (4)$$

$$NADH^{\bullet+} \rightarrow NAD^{+} + H^{\bullet} \qquad \Delta H_{homo}(NADH^{\bullet+}) = ? \qquad (5)$$

we have successfully developed four new thermodynamic cycles according to the reactions of the *N*,*N*,*N*′,*N*′-tetramethyl-*p*-phenylenediamine radical cation with some NADH models in acetonitrile; these can be used to directly evaluate the bond dissociation energies of the C4–H bonds in NADH models and their radical cations. Here we report the details.

Results

N,*N*,*N*′,*N*′-Tetramethyl-*p*-phenylenediamine radical cation perchlorate ($TMPA^{\bullet+}ClO_4^{-}$) is a very strong single-electron organic oxidant,[14] which can readily oxidise NADH models such as 1-benzyl-1,4-dihydronicotinamide (BNAH), Hantzsch 1,4-dihydropyridine (HEH), 10-methyl-9,10- dihydroacridine ($AcrH_2$), and many other 1,4-dihydropyridine derivatives in acetonitrile to give *N*,*N*,*N*′,*N*′-tetramethyl-*p*-phenylenediamine and the corresponding pyridinium cation derivatives, respectively. The stoichiometry of the reactions was determined by using spectrophotometric titration (see Figure 1).

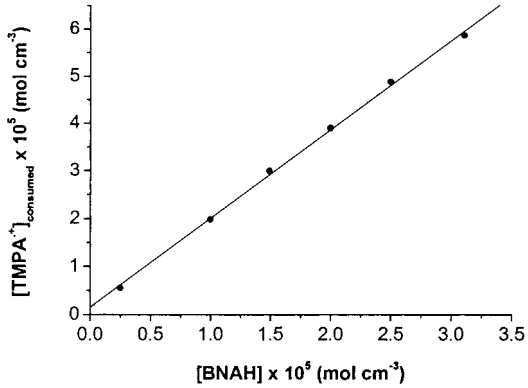

Figure 1. Plot of the concentration of $TMPA^{\bullet+}$ consumed in the electron-transfer reactions of BNAH with $TMPA^{\bullet+}$ versus the concentration of BNAH.

The results showed that two moles of $TMPA^{\bullet+}$ were required to thoroughly consume one mole of NADH models such as BNAH in dry acetonitrile [Eq. (6)]. The reaction mechanism was proposed to be an $e^{-}-H^{+}-e^{-}$ sequence of hydride transfer (Scheme 2).[15]

On the basis of the reaction [Eq. (6)], four thermodynamic cycles were constructed as shown in Schemes 3 and 4, from which four formulae to evaluate the heterolytic and homolytic C4–H bond dissociation energies in NADH models and their radical cations were derived [Eqs. (7) and (8) from the cycles in Scheme 3 and Eqs. (9) and (10) from the cycles in Scheme 4].[16] From Equations (7)–(10), the heterolytic and homolytic bond dissociation energies of the C4–H bonds in NADH models and their radical cations can be easily

0947-6539/03/0904-0872 $ 20.00+.50/0 *Chem. Eur. J.* **2003**, *9*, No. 4

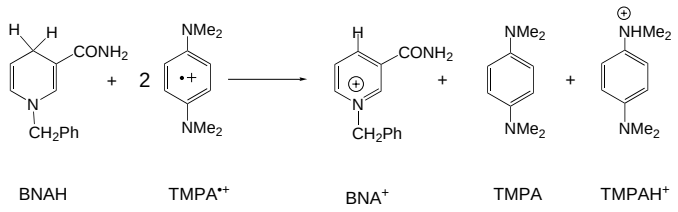

(6)

electron transfer	$BNAH + TMPA^{\bullet+} \rightarrow BNAH^{\bullet+} + TMPA$
proton transfer	$BNAH^{\bullet+} + TMPA \rightarrow BNA^{\bullet} + TMPAH^{+}$
electron transfer	$BNA^{\bullet} + TMPA^{\bullet+} \rightarrow BNA^{+} + TMPA$
The net reaction result	$BNAH + 2TMPA^{\bullet+} \rightarrow BNA^{+} + TMPA + TMPAH^{+}$

Scheme 2. Reaction mechanism of BNAH with $TMPA^{\bullet+}$.

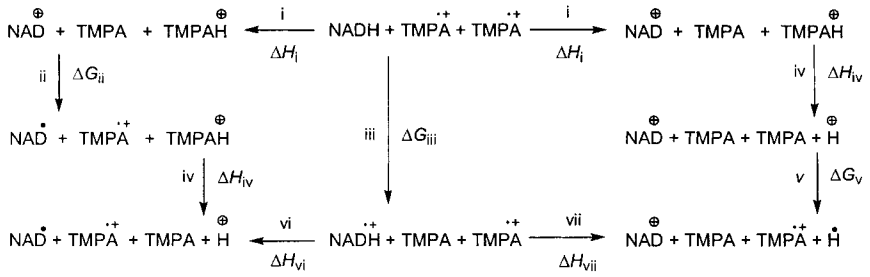

Scheme 3. Two thermodynamic cycles constructed from the reactions of $TMPA^{\bullet+}$ with NADH Models. i) $\Delta H_i = \Delta H_{rxn}$. ii) $\Delta G_{ii} = -F[E_{1/2}(NAD^+) - E_{1/2}(TMPA^{\bullet+})]$. iii) $\Delta G_{iii} = -F[E_{1/2}(TMPA^{\bullet+}) - E_{1/2}(NADH)]$. iv) $\Delta H_{iv} = \Delta H_a(TMPAH^+)$. v) $\Delta G_v = -F[E_{1/2}(H^{+/0}) - E_{1/2}(TMPA^{\bullet+})]$. vi) $\Delta H_{vi} = \Delta H_{het}(NADH^{\bullet+})$. vii) $\Delta H_{vii} = \Delta H_{homo}(NADH^{\bullet+})$

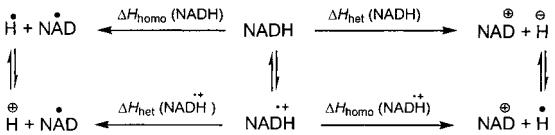

Scheme 4. Two thermodynamic cycles were made on the basis of the heterolytic and homolytic $(C4–H)^{\bullet+}$ bond dissociations in the radical cations of NADH models.

obtained only if the enthalpy change of the reaction [Eq. (6)] (ΔH_{rxn}), the enthalpy change of deprotonation of $TMPAH^+$ [$\Delta H_a(TMPAH^+)$], and the redox potentials of the related species are available. Evidently, the enthalpy changes can be obtained from the corresponding heats of reaction, which can be directly determined by titration calorimetery. The redox potentials can be measured by cyclic voltammetry.

$$\Delta H_{homo}(NADH^{\bullet+}) = F[E_{1/2}(TMPA^{\bullet+}) - E_{1/2}(NADH)] - F[E_{1/2}(H^{+/0}) - E_{1/2}(TMPA^{\bullet+})] + \Delta H_a(TMPAH^+) + \Delta H_{rxn} \quad (7)$$

$$\Delta H_{het}(NADH^{\bullet+}) = F[E_{1/2}(TMPA^{\bullet+}) - E_{1/2}(NADH)] - F[E_{1/2}(NAD^+) - E_{1/2}(TMPA^{\bullet+})] + \Delta H_a(TMPAH^+) + \Delta H_{rxn} \quad (8)$$

$$\Delta H_{het}(NADH) = \Delta H_{homo}(NADH^{\bullet+}) - F[E_{1/2}(H^{0/-}) - E_{1/2}(NADH)] \quad (9)$$

$$\Delta H_{homo}(NADH) = \Delta H_{het}(NADH^{\bullet+}) - F[E_{1/2}(H^{+/0}) - E_{1/2}(NADH)] \quad (10)$$

Three types of 1,4-dihydropyridine derivatives were chosen as NADH models in this work; these include seven 1,4-dihydronicotinamide derivatives (**1**), two Hantzsch 1,4-dihydropyridine derivatives (**2**), and 9,10-dihydroacridine derivatives (**3**) (Scheme 5).

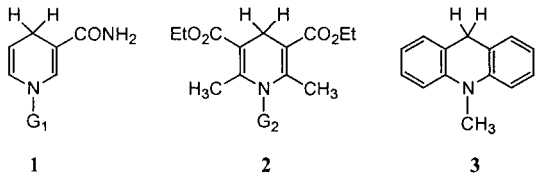

Scheme 5. **1**: $G_1 = PhCH_2$ (BNAH), 4-CH_3OPh (CH_3OPNAH), 4-CH_3Ph (CH_3PNAH), Ph (PNAH), 4-ClPh (ClPNAH), 4-BrPh (BrPNAH), 4-CF_3Ph (CF_3PNAH). **2**: $G_2 = H$ (HEH), CH_3 (MeHEH). **3**: $AcrH_2$.

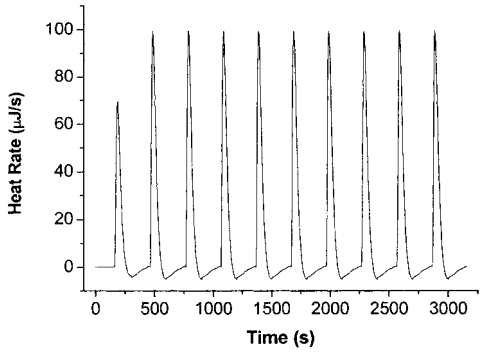

Figure 2. Titration calibration graph: BNAH in acetonitrile was titrated into *N*,*N*,*N*′,*N*′-tetramethyl-*p*-phenylenediamine radical cation ($TMPA^{\bullet+}$) in acetonitrile solution ([BNAH] = 2.01 mM, $[TMPA^{\bullet+}]$ = 10.87 mM).

The titration calorimetry was performed in acetonitrile at 25 °C on a CSC4200 isothermal titration calorimeter taking 10 automatic injections; the reaction heats were obtained by area integration of each peak except the first one (calibration graph, see Figure 2). The ten enthalpy changes of the reaction [Eq. (6)] (ΔH_{rxn}) and the deprotonation enthalpy change of $TMPAH^+$ [$\Delta H_a(TMPAH^+)$] in acetonitrile, as well as redox potentials of $TMPA^{\bullet+}$, NADH, and NAD^+ models are listed in Table 1. Heterolytic and homolytic C4–H bond dissociation energies for the ten NADH models and the corresponding ten radical cations are summarized in Table 2; these data provide a good platform for the comparison of the relative ease with which the C4–H bond scission processes among the different types of NADH models and their radical cations take place. The stabilities of the related reactive intermediates can also be visualized on the basis of the derived energetic data.

Table 1. Reaction enthalpy changes of the NADH models with *N*,*N*,*N*′,*N*′-tetramethyl-*p*-phenylenediamine radical cation perchlorate ($TMPA^{\bullet+}$) and the redox potentials [V versus $Fc^{+/0}$] of the relative species in acetonitrile.

NADH Models	ΔH_{rxn}[a]	E_{ox}(NADH)[b]	$E_{red}(NAD^+)$[b]	$E_{1/2}$(TMPA)[b]	$\Delta H_a(TMPAH^+)$[c]
1					
BNAH	−38.0	0.259	−1.297	0.296	9.1
CH_3OPNAH	−35.3	0.281	−1.247	0.296	9.1
CH_3PNAH	−34.6	0.313	−1.209	0.296	9.1
PNAH	−33.4	0.363	−1.154	0.296	9.1
ClPNAH	−31.9	0.395	−1.087	0.296	9.1
BrPNAH	−31.7	0.400	−1.082	0.296	9.1
CF_3PNAH	−29.6	0.471	−1.003	0.296	9.1
2					
HEH	−32.9	0.507	−1.142	0.296	9.1
MeHEH	−32.3	0.498	−1.089	0.296	9.1
3					
$AcrH_2$	−21.1	0.492	−0.819	0.296	9.1

[a] ΔH_{rxn} obtained from the reaction heat of Equation (6) by switching the sign of the heat value, the latter was measured by titration calorimetry in MeCN at 25 °C. The data given in kcal mol^{-1} were average values of at least two independent runs, each of which was again an average value of ten consecutive titrations, except the first. The reproducibility is 0.5 ± 0.2 kcal mol^{-1}. [b] Measured in MeCN at 25 °C in volts by mV versus $Fc^{+/0}$ and reproducible to 5 mV or better. [c] $\Delta H_a(TMPAH^+)$ is the enthalpy change of the deprotonation of $TMPAH^+$ equal to the reaction heat of TMPA with $HClO_4$ in acetonitrile, the latter was measured by titration calorimetry at 25 °C. The data [kcal mol^{-1}] obtained were average values of two independent runs, each of which was again an average value of 10 consecutive titrations except the first. Uncertainty is smaller than 0.6 kcal mol^{-1}.

Table 2. Heterolytic and homolytic C4–H bond dissociation energies of the NADH models and their radical cations in acetonitrile [kcal mol^{-1}].[a]

NADH Models	ΔH_{het}(NADH)	ΔH_{homo}(NADH)	$\Delta H_{het}(NADH^{\bullet+})$	$\Delta H_{homo}(NADH^{\bullet+})$
1				
BNAH	64.2	67.9	8.7	32.0
CH_3OPNAH	66.9	69.4	9.7	34.2
CH_3PNAH	67.5	69.2	8.8	34.1
PNAH	68.8	69.2	7.6	34.2
ClPNAH	70.2	69.1	6.8	34.9
BrPNAH	70.4	69.2	6.8	35.0
CF_3PNAH	72.6	69.5	5.4	35.5
2				
HEH	69.3	69.4	4.5	31.4
MeHEH	69.9	68.8	4.1	32.2
3				
$AcrH_2$	81.1	73.7	9.2	43.5

[a] ΔH_{het}(NADH), ΔH_{homo}(NADH), $\Delta H_{het}(NADH^{\bullet+}$ and $\Delta H_{homo}(NADH^{\bullet+})$ were estimated from Equations (7)–(10), taking $E_{1/2}(H^{+/0}) = -2.307$ (V versus $Fc^{+/0}$), $E_{1/2}(H^{0/-}) = -1.137$ [V versus $Fc^{+/0}$] (the values from Parker's work[24] adjusted to versus $Fc^{+/0}$ by adding −0.537 V). Standard deviations were estimated to be smaller than 1 kcal mol^{-1}.[17]

Discussion

Heterolytic and homolytic bond dissociation energies of the C4–H bonds in the NADH models and the relative stabilities of the corresponding pyridinium cation and pyridinyl radical: The second column in Table 2 shows that the energetic scale of the heterolytic bond dissociation of the C4–H bonds in the ten NADH models in acetonitrile ranges from 64.2 kcal mol^{-1} for BNAH to 81.1 kcal mol^{-1} for $AcrH_2$. This is much smaller than the hydride affinities of the primary benzylic carbenium ion in acetonitrile (e.g., the hydride affinities of 118, 106, 112, 122, 121, and 122 kcal mol^{-1} for $PhCH_2^+$, 4-$CH_3OC_6H_4CH_2^+$, 4-$MeC_6H_4CH_2^+$, 4-$FC_6H_4CH_2^+$, 4-$ClC_6H_4CH_2^+$, and 4-$CNC_6H_4CH_2^+$, respectively),[18] but close to the hydride affinities of some transition-metal hydrides in acetonitrile (e.g., the hydride affinities of 66.2 and 60.4 kcal mol^{-1} for $[HNi(depp)_2]^+$ and $[HNi(dmpp)_2]^+$, respectively; depp = bis(diethylphosphino)propane, dmpp = bis(dimethylphosphino)propane);[19] this suggests that the NADH models with the 1,4-dihydropyridine structure would be a good hydride donor reducing agent, which fits well with many other experimental results.[4] The reason could be that the pyridinium salts formed by the heterolytic C4–H bond dissociation are more stable than the primary benzylic carbenium ions in acetonitrile. This result may provide a reason why NADH coenzyme chooses 1,4-dihydropyridine as its reaction active center in vivo. Detailed examination of the heterolytic bond dissociation energies of the C4–H bonds in BNAH, HEH, and $AcrH_2$ (as three typical NADH models) reveals that the magnitude of the heterolytic bond dissociation energies of the C4–H bonds increases in the following order of NADH models: BNAH (64.2 kcal mol^{-1}) < HEH (69.3 kcal mol^{-1}) < $AcrH_2$ (81.1 kcal mol^{-1}); this is an indication that BNAH should be the strongest hydride donor, while $AcrH_2$ should be the weakest hydride contributor among the three NADH models. This has been supported by many experiments.[3–6]

To verify the heterolytic bond dissociation energies of the C4–H bonds in the NADH models obtained using the present method, the reaction heats of $AcrH^+$ with NADH models **1** and **2** in acetonitrile were determined. The results are summarized in Table 3. Since a hydride exchange completed the reactions of $AcrH^+$ with **1** and **2** [Eq. (11)],[20] the reaction heats (Q_{rxn}) should be equal to the difference of the heterolytic C4–H bond dissociation energies between $AcrH_2$ and **1** and **2**. Evidently, the differences between ΔH_{het}(**1**,**2**) and $\Delta H_{het}(AcrH_2)$ in Table 3 are well matched with the corresponding reaction heats; this suggests that the heterolytic bond dissociation energies of the C4–H bonds in the NADH models obtained by the present method should be reliable, and also supports the efficiency of the present method.

From the third column in Table 2, the energetic scale of the homolytic bond dissociation of the C4–H bonds in the ten NADH models in acetonitrile ranges from 67.9 kcal mol^{-1} for BNAH to 73.7 kcal mol^{-1} for $AcrH_2$, which is smaller than the

0947-6539/03/0904-0874 $ 20.00+.50/0 *Chem. Eur. J.* **2003**, *9*, No. 4

Table 3. The differences between $\Delta H_{het}(AcrH_2)$ and $\Delta H_{het}(NADH)$ along with the reaction heats (Q_{rxn}) of $AcrH^+$ with the other NADH models in acetonitrile [kcal mol^{-1}].

NADH Models	$\Delta H_{het}(AcrH_2) - \Delta H_{het}(NADH)$	Q_{rxn}[a]
BNAH	16.9	16.6
CH_3OPNAH	14.2	14.7
CH_3PNAH	13.6	13.6
PNAH	12.3	12.0
ClPNAH	10.9	10.5
BrPNAH	10.7	10.3
CF_3PNAH	8.5	8.9
HEH	11.8	11.6
MeHEH	11.2	11.0

[a] Q_{rxn} denoting the reaction heat of $AcrH^+$ with the NADH models **1**, **2** [Eq. (11)] measured by titration calorimetry in CH_3CN at 25 °C. The data obtained were average values of at least two independent runs, each of which was again an average value of ten consecutive titrations except the first. The reproducibility is 0.5 ± 0.2 kcal mol^{-1}.

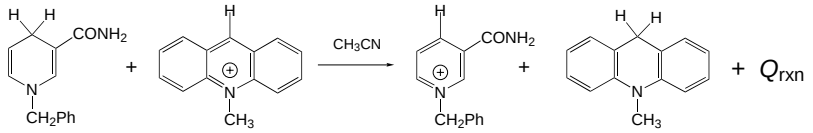

(11)

bond dissociation energies (BDE) of 9-substituted fluorenes (Fl-H) in dimethyl sulfoxide[21] (e.g., the BDEs of 76.0, 74.0, and 82.1 kcal mol^{-1} for 9-CO_2Me-Fl-H, 9-Ph-Fl-H, and Fl-H, respectively),[22, 23] but close to the M–H BDE of some metal hydrides in acetonitrile, which is a good hydrogen-atom donor (such as the BDE's of 61.5, 69.2, 72.3, 57.1, and 64.9 kcal mol^{-1} for ([(η^5-C_5H_5)Cr(CO)$_3$H], [(η^5-C_5H_5)Mo(CO)$_3$H], [(η^5-C_5H_5)W(CO)$_3$H], [(η^5-C_5H_5)Fe(CO)$_2$H], and [(η^5-C_5H_5)Ru-(CO)$_2$H], respectively).[24] These results suggest that the three types of NADH models (**1**, **2**, **3**) are not only good hydride donors, but also good hydrogen-atom contributors. This is supported by their reactions with some organic bromides[25] and peroxides.[26] Meanwhile, the low homolytic C4–H bond dissociation energies hint that the pyridinyl radicals NAD$^\bullet$ formed by homolytic C4–H bond dissociation from the NADH models should not be too unstable in acetonitrile solution: they would be able to be captured by diamagnetic radical scavengers (spin traps) or other reactive radicals; this, in fact, has been confirmed by extensive experimental results.[27] Comparison of columns 2 and 3 in Table 2 shows that when the NADH model is BNAH, the ΔH_{homo} of the C4–H bond is larger than the corresponding ΔH_{het} by 3.7 kcal mol^{-1}, but when the NADH model is $AcrH_2$, the ΔH_{homo} of the C_9–H bond is smaller than the corresponding ΔH_{het} by 7.4 kcal mol^{-1}. This suggests that if BNAH is used as the NADH model to react with an oxidant, initial hydride transfer should be more likely than the initial hydrogen atom transfer, but if $AcrH_2$ is used as the NADH model, the case is reversed; this has been also supported by many other reports.[2–6] Examining the ΔH_{het} (69.3 kcal mol^{-1}) and ΔH_{homo} (69.4 kcal mol^{-1}) of the C4–H bond for HEH shows that the ΔH_{het} and ΔH_{homo} are close to each other; this indicates that the hydride and hydrogen-atom transfer from HEH is almost equally possibile. In addition, by detailed inspection of the relationship of ΔH_{het}(NADH) and ΔH_{homo}(NADH) for the 1-aryl-1,4-dihydronicotinamide GPNAH, it is interesting to find that when the substituent G is an electron-donating group (EDG), the heterolytic bond dissociation energies of the C4–H bonds are smaller than the corresponding homolytic bond dissociation energies of the C4–H bonds, but when the substituent G is an electron-withdrawing group (EWG), the ΔH_{het}(NADH) becomes larger than the corresponding ΔH_{homo}(NADH). This result suggests that when the substituent G is an EDG, the NADH model has better hydride-donating properties than when G is an EWG, but when the G is an EWG, the NADH model become a better donor of hydrogen atoms than when the substituent is an EDG. Clearly, whether the hydride or the hydrogen atom is more likely to be released from 1-aryl-1,4-dihydronicotinamide can be controlled by changing the remote substituent G.

Heterolytic and homolytic bond dissociation energies of the (C4–H)$^{\bullet+}$ bonds in the NADH$^{\bullet+}$ models: As stated in the introduction section, there are many chemical mimic experiments that support the idea that the reactions of the NADH models were initiated by a single-electron transfer.[5, 28] It is well recognized that if the reaction of NADH is initiated by a single-electron transfer, an incipient radical cation intermediate NADH$^{\bullet+}$ should be formed from which a proton transfer or a hydrogen-atom transfer is believed to follow in the second reaction step. So, the question arises as to which species (hydride or hydrogen atom) is more likely to transfer in the second reaction step. Clearly, it is necessary to evaluate and compare the heterolytic and homolytic bond dissociation energies of the (C4–H)$^{\bullet+}$ bonds in the radical cations of the NADH models. From columns 4 and 5 in Table 2, we find that the energetic scale of the heterolytic bond dissociation of the (C4–H)$^{\bullet+}$ bonds in the nine NADH$^{\bullet+}$ models in acetonitrile ranges from 4.1 kcal mol^{-1}, for the radical cation of *N*-methylated Hantzsch 1,4-dihydropyridine, to 9.7 kcal mol^{-1}, for the radical cation of 1-(*para*-methoxylphenzyl)-1,4-dihydronicotinamide. The energetic scale of the corresponding homolytic bond dissociation of the (C4–H)$^{\bullet+}$ bonds ranges from 31.4 kcal mol^{-1} for HEH$^{\bullet+}$ to 43.5 kcal mol^{-1} for $AcrH_2^{\bullet+}$. Clearly, a simple comparison of the heterolytic (C4–H)$^{\bullet+}$ bond cleavage energies with the corresponding homolytic (C4–H)$^{\bullet+}$ bond cleavage energies reveals that the heterolytic (C4–H)$^{\bullet+}$ bond cleavage energies are quite a bit smaller than the corresponding homolytic (C4–H)$^{\bullet+}$ bond cleavage energies, in fact by 23.3 – 34.3 kcal mol^{-1}. This indicates that the proton transfer from the NADH$^{\bullet+}$ models should be much easier than the hydrogen-atom transfer from the same NADH$^{\bullet+}$ models. From the very low heterolytic bond dissociation energies of the (C4–H)$^{\bullet+}$ bonds (4.1 – 9.7 kcal mol^{-1}), it is conceivable that the proton transfer should be extremely fast and is possibly diffusion-controlled in solution. Here it is concluded that the $e^- - H^+ - e^-$ sequence of hydride transfer should be the most likely among all the possible multi-step hydride-transfer mechanisms of NADH and its models.

  0947-6539/03/0904-0875 $ 20.00+.50/0

Examination of the heterolytic bond dissociation energies of the (C4–H)$^{\bullet+}$ bonds among the three extensively used NADH models (BNAH, HEH, and $AcrH_2$) shows that $HEH^{\bullet+}$ (4.5 kcal mol^{-1}) is the strongest acid among the three $NADH^{\bullet+}$ models. Inspection of the homolytic bond dissociation energies of the (C4–H)$^{\bullet+}$ bonds in BNAH, HEH, and $AcrH_2$ reveals that $HEH^{\bullet+}$ (31.4 kcal mol^{-1}) is the strongest hydrogen donor, whereas $AcrH_2^{\bullet+}$ (43.5 kcal mol^{-1}) is the weakest hydrogen contributor, which is also in line with many experimental results. In fact, the radical cation $AcrH_2^{\bullet+}$ can be directly detected and characterized by EPR spectroscopy,[29] but so far the radical cations $BNAH^{\bullet+}$ and $HEH^{\bullet+}$ cannot.

Driving-force analysis on each mechanistic step of hydride transfer from the NADH models oxidized by $TMPA^{\bullet+}$: Extensive chemical mimic experimental results show that the 4-hydrogen was transferred by the $e^- - H^+ - e^-$ mechanism in the reactions of NADH models with one-electron oxidants. However, which of the three elementary steps is the rate-limiting step is still a disputed question. Some reports insist that the initial electron transfer should be the rate-limiting step according to the observation of no remarkable kinetic isotopic effect,[4d, 30] others argue that the second proton transfer should be the rate-limiting step on the basis of general base catalysis.[5f, 31] Clearly, it is necessary to invoke thermodynamic driving force analysis on each mechanistic step to aid solution of the mechanistic problem. Regarding the reaction mechanism of the nine NADH models with $TMPA^{\bullet+}$ as mentioned above, the 4-hydrogen transfer from the NADH models should proceed in an $e^- - H^+ - e^-$ three-step sequence.[15] However, it is difficult to determine which is the rate-limiting step. In order to solve this problem, the driving force for each elementary step in Scheme 2 has been calculated according to the thermodynamic data obtained in this work; the details are listed in Table 4.

The most eye-catching feature of the data in Table 4 is that the energy changes of all the elementary steps are either exothermic or only slightly endothermic, indicating that oxidation of the nine NADH models by $TMPA^{\bullet+}$ would readily take place and quickly go to completion. The experimentally observed clean and rapid reactions in this work do in fact support this expectation based on the energetic analysis. Detailed inspection of the last three columns in Table 4 shows that the free-energy changes of electron transfer in the third reaction step for the nine reactions are all very large negative values (−25.7 to −36.7 kcal mol^{-1}), which indicate that the electron transfer in the third reaction step for the nine reactions would be diffusion-controlled. The rate-limiting step is therefore either the initial electron transfer or the second proton transfer. By comparing the free-energy changes in the first two reaction steps, it is clear that when the NADH model is BNAH and CH_3OPNAH (group I in Table 4), the driving forces of the initial electron transfer are larger than the corresponding driving forces of the proton transfer in the second step. This suggests that the proton transfer in the second step could be the rate-limiting step. However, for group II, the driving forces of the initial electron transfer are quite a bit smaller than those of the corresponding proton transfer in the second step; this suggests that the initial electron transfer could be the rate-limiting step. Though these suggestions have not been verified by other experimental results, the mechanistic guidelines suggested here should be valuable in predicting or differentiating the mechanistic possibilities of NADH model reactions.

Evaluation of the effective charge distribution on the pyridine ring in the models of NADH, $NADH^{\bullet+}$, $NAD^{\bullet}$, and NAD^+: $NADH^{\bullet+}$ and $NAD^{\bullet}$ are important intermediates formed during the course of NADH reduction initiated by one-electron transfer; however, very little information about the structure and the charge distribution is available. In order to elucidate the structure and the charge distribution on the pyridine ring, the dependencies of ΔH_{het}(GPNAH), ΔH_{homo}($GPNAH^{\bullet+}$), and ΔH_{het}($GPNAH^{\bullet+}$) on the substituent constant (σ) were examined (see Figure 3). This exhibits three

Table 4. Energetics (kcal mol^{-1}) of each mechanistic step for the reactions of $TMPA^{\bullet+}$ with the NADH models in acetonitrile shown in Scheme 2.

Models	$e^- - H^+ - e^-$		
	ΔG(eT)[a]	$\Delta H(H^+T)$[b]	$\Delta G'$(eT)[c]
Group I			
BNAH	−0.9	−0.4	−36.7
CH_3OPNAH	−0.4	0.6	−35.6
Group II			
CH_3PNAH	0.4	−0.3	−34.7
PNAH	1.6	−1.5	−33.4
ClPNAH	2.3	−2.3	−31.9
BrPNAH	2.4	−2.3	−31.8
CF_3PNAH	4.0	−3.7	−30.0
HEH	4.9	−4.6	−33.2
MeHEH	4.7	−5.0	−31.9
$AcrH_2$	4.5	−0.1	−25.7

[a] Calculated according to the equation of $\Delta G(eT) = -23.06[E_{1/2}(TMPA^{\bullet+}) - E_{ox}(NADH)]$. [b] Calculated from the equation of $\Delta H(H^+T) = \Delta H_{het}(NADH^{\bullet+}) - \Delta H_a(TMPAH^+)$. [c] Calculated according to the equation of $\Delta G'(eT) = -23.06[E_{1/2}(TMPA^{\bullet+}) - E_{red}(NAD^+)]$.

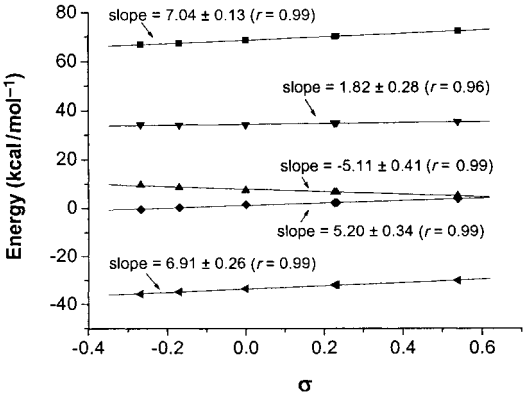

Figure 3. Hammett plots of ΔH_{het}(NADH) (■), ΔH_{homo}($NADH^{\bullet+}$) (▼), ΔH_{het}($NADH^{\bullet+}$) (▲), ΔG(eT) (◆), and $\Delta G'$(eT) (◀) versus σ. NADH = GPNAH (G = 4-OCH_3, 4-CH_3, 4-H, 4-Cl, 4-Br, 4-CF_3). ΔH_{het}(NADH), ΔH_{het}($NADH^{\bullet+}$), and ΔH_{homo}($NADH^{\bullet+}$) are listed in Table 2; ΔG(eT) and $\Delta G'$(eT) were calculated according to the equations $\Delta G(eT) = -23.06[E_{1/2}(TMPA^{\bullet+}) - E_{ox}(GPNAH)]$ and $\Delta G'(eT) = -23.06[E_{1/2}(TMPA^{\bullet+}) - E_{red}(GPNA^+)]$, respectively.

0947-6539/03/0904-0876 $ 20.00+.50/0 *Chem. Eur. J.* **2003**, *9*, No. 4

lines with slopes of 7.04 ± 0.13 (equivalent to ρ of -1.235 for the heterolytic C4–H bond scission reaction),[32] 1.82 ± 0.28 (equivalent to ρ of -0.319 for the homolytic $(C4–H)^{\bullet+}$ bond scission reaction), and -5.11 ± 0.41 (equivalent to the ρ of 0.896 for the heterolytic $(C4–H)^{\bullet+}$ bond scission reaction). The positive slopes for ΔH_{het}(GPNAH) and $\Delta H_{homo}(GPNAH^{\bullet+})$ against the substituent constant σ reflect that the positive charge increases at the N1 atom on the pyridine ring in going from GPNAH to $GPNA^+$, and from $GPNAH^{\bullet+}$ to $GPNA^+$, respectively. The negative slope for $\Delta H_{het}(GPNAH^{\bullet+})$ reflects the positive charge decrease on the N1 atom in going from $GPNAH^{\bullet+}$ to $GPNA^{\bullet}$. The magnitude of the line slope values is a measure of the effective charge change on the N1 atom. Comparing the magnitudes of the three slope values for ΔH_{het}(GPNAH), $\Delta H_{homo}(GPNAH^{\bullet+})$, and $\Delta H_{het}(GPNAH^{\bullet+})$ shows that the absolute values of the three slopes are |slope for ΔH_{het}(GPNAH)| > |slope for $\Delta H_{het}(GPNAH^{\bullet+})$| > |slope for $\Delta H_{homo}(GPNAH^{\bullet+})$|, indicating that the effective change in charge on the N1 atom would decrease in the following order: GPNAH (heterolytic) > $GPNAH^{\bullet+}$ (heterolytic) > $GPNAH^{\bullet+}$ (homolytic). In order to quantitatively evaluate the relative effective charge changes on the N1 atom for the three different C4–H bond dissociation processes, we arbitrarily defined that the effective charge on the N1 atom in GPNAH is zero, and the effective charge on the N1 atom in the $GPNA^+$ is a *positive one*. This is from our basic knowledge of the electronic structures of the neutral GPNAH and the corresponding quaternary ammonium salts $GPNA^+$; these indicate that the slope value of 7.04 for the heterolytic C4–H bond scission process is equivalent to a positive charge increase of one unit on the N1 atom in going from GPNAH to $GPNA^+$. According to this definition, it is clear that the slope of 1.82 ± 0.28 for $\Delta H_{homo}(GPNAH^{\bullet+})$ is equivalent to the positive charge increase of 0.259 ± 0.039 on the N1 atom on going from $GPNAH^{\bullet+}$ to $GPNA^+$. Since the effective charge on the N1 atom in $GPNA^+$ has been defined as a *positive one*, the effective charge on the N1 atom in $GPNAH^{\bullet+}$ should be 0.741 ± 0.039 (Scheme 6). Similarly, the slope of -5.11 ± 0.41 for $\Delta H_{het}(GPNAH^{\bullet+})$ should be equivalent to the negative effective charge increase of -0.726 ± 0.058 on the N1 atom on going from $GPNAH^{\bullet+}$ to $GPNA^{\bullet}$. This suggests that the N1 atom in $GPNA^{\bullet}$ should possess an effective charge of 0.015 ± 0.058 according to the effective charge of 0.741 on the N1 atom in $GPNAH^{\bullet+}$ ascertained above. In order to further support the evaluations made above, the Hammett-type linear free-energy correlations of ΔG(eT) and $\Delta G'$(eT) against the substituent constant (σ) were also performed (see Figure 3). The line slopes are 5.20 ± 0.34 and 6.91 ± 0.24 for ΔG(eT) and $\Delta G'$(eT), respectively, which is equivalent to the positive charge increases of 0.739 ± 0.048 and 0.982 ± 0.034 on the N1 atom on going from GPNAH to $GPNAH^{\bullet+}$ and from $GPNA^{\bullet}$ to $GPNA^+$, respectively (Scheme 6). Clearly, the effective charge changes of 0.739 and 0.982 are close to the differences of the corresponding effective charges on the N1 atom between PNAH (0.000) and $GPNAH^{\bullet+}$ (+0.741), and between $GPNA^{\bullet}$ (0.015) and $GPNA^+$ (+1.000), respectively. The deviations are all within the experimental errors, suggesting that the evaluations of the effective charge on the N1 in the $GPNAH^{\bullet+}$ and $GPNA^{\bullet}$ derived from the slope values of the Hammett-type free-energy linear plots are reasonable and reliable. In fact, similar evaluations of effective charge distribution on an active atom in a molecule or a transition-state structure by using the Hammett linear free-energy relationship have been extensively reported in the literature.[33] According to the evaluation of the effective charge (+0.741) on the 1-position nitrogen in $GPNAH^{\bullet+}$, it is conceived that the center of the radical spin in $GPNAH^{\bullet+}$ should be located at the carbon atoms on the pyridine ring. The resonance structures of $GPNAH^{\bullet+}$ (Scheme 7) show that the 3- or 5-position carbon on the pyridine ring should be the spin center, but only the latter was supported by the formation of the [2+3] cycloadduct of BNAH with *p*-benzoquinone initiated by single-electron transfer.[34] Concerning the pyridinyl radical $GPNA^{\bullet}$, the evaluation of 0.015 positive effective charge on the N1 atom suggests that the lone pair of electrons remains on N1 in $GPNA^{\bullet}$, indicating that the single electron should appear mainly on the 4-position carbon atom (see the resonance structures for $GPNA^{\bullet}$ in Scheme 7). That is, radical $GPNA^{\bullet}$ should be essentially due to a carbon radical rather than a hetero-atom-centered radical; this has been supported by many experimental results.[35] According to the effects of the *para*-substituents (G) on the BDEs of the C4–H bond in GPNAH (see the third column in Table 2), it is interesting to find that the pyridinyl radical of $GPNA^{\bullet}$ is destabilized not only by the remote electron-donating substituents (EDG), but also by the remote electron-withdrawing substituents (EWG); this differs substantially from the previously reported behaviors of carbon radicals in the literature in which both the EDGs and EWGs were found to be radical-stabilizing (i.e., the so-called "Class S" radical).[36] This also differs from the observations on various kinds of heteroatom-centered radicals so far investigated, which show "O (opposite)-type" substituent behavior, that is, EDG is radical-stabilizing

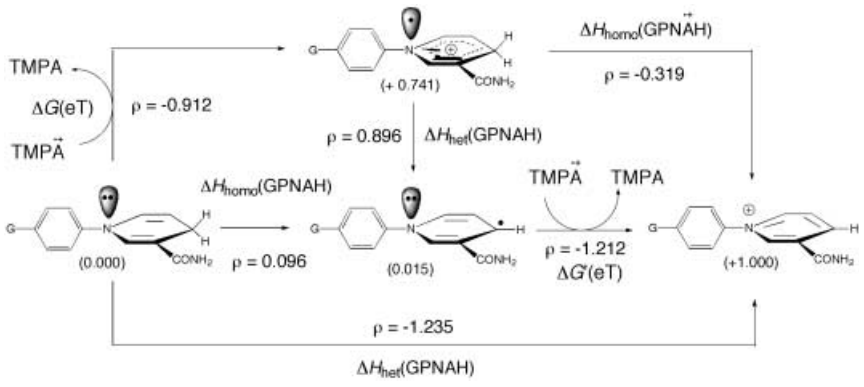

Scheme 6. Relative effective charge on the 1-position nitrogen atom (N-1) in GPNAH, $GPNAH^{\bullet+}$, $GPNA^{\bullet}$, and $GPNA^+$ in acetonitrile.

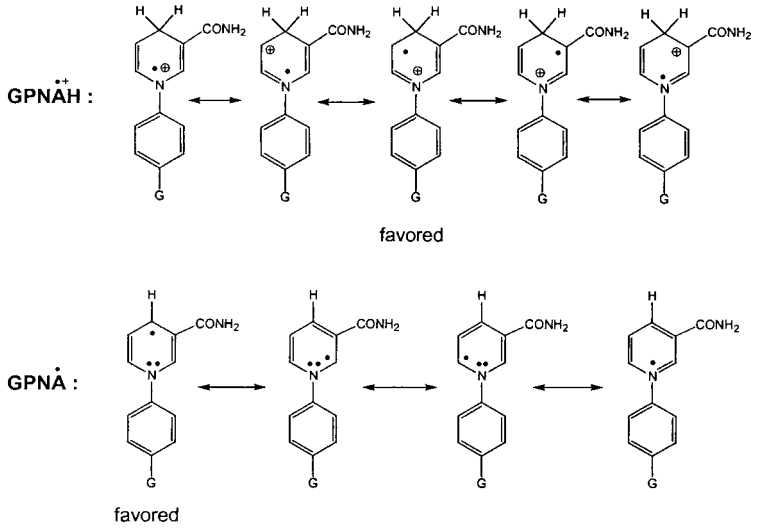

Scheme 7. Resonance structures of GPNAH$^{\bullet+}$ and GPNA$^{\bullet}$.

but EWG is radical-destabilizing (so-called "Class O" radical).[37] On the basis of the earlier so-called class S/O radical definition of Walter,[37a] the pyridinyl radical GPNA$^{\bullet}$ should be a class counter-S type, which suggests that not all carbon radicals have S-type behavior.

Conclusions

Four sets of C4–H bond dissociation energies for ten NADH models and their radical cations were determined in acetonitrile by a new, developing method. It can be concluded that:

1) The heterolytc and homolytic C4–H bond scission energies for the ten NADH models are significantly smaller than those of general sp^3 C–H bonds; this suggests that the NADH models should be not only good hydride donors but also good hydrogen-atom contributors in solution.
2) When the NADH model is 1-benzyl-1,4-dihydronicotinamide (BNAH), the heterolysis of the C4–H bond to release a hydride is more likely to take place than the corresponding homolysis to remove a hydrogen atom in solution; when the NADH model is 9,10-dihydroacridine ($AcrH_2$), the homolysis of the C_9–H bond to remove a hydrogen atom is more likely to take place than the corresponding heterolysis of the C_9–H bond to release a hydride in solution. However, when the NADH model is Hantzsch 1,4-dihydropyridine (HEH), the hydride and hydrogen-atom transfers from HEH occur with almost equal probability.
3) Since the ΔH_{het}(NADH$^{\bullet+}$) for the ten NADH models are much smaller than the corresponding ΔH_{homo}(NADH$^{\bullet+}$), it is conceived that the $e^- - H^+ - e^-$ sequence of hydride transfer should be the most likely among all the possible multi-step hydride transfer mechanisms of NADH and its models.
4) The pyridinyl radical GPNA$^{\bullet}$ should be due to a counter-S type carbon radical rather than a nitrogen radical and the lone single electron mainly appears at the C4-position on the pyridine ring.
5) Hammett-type linear free-energy analyses show that the N1 atom on the pyridine ring carries the relative effective charges of 0.000, +0.741, 0.015, and +1.000 in GPNAH, GPNAH$^{\bullet+}$, GPNA$^{\bullet}$, and GPNA^{+}, respectively, which, to our best knowledge, appears to be the first work to quantitatively and experimentally evaluate the relative effective charge distribution on the N1 atom in the various forms of NADH model GPNAH.

Experimental Section

Materials: 1-Benzyl-1,4-dihydronicotinamide (BNAH) was prepared according to the literature method.[38] Hantzsch 1,4-dihydropyridine was prepared by depositing the mixture of aldehyde, ammonia, and ethyl acetoacetate in methanol. *N*-Methylated Hantzsch 1,4-dihydropyridines were prepared according to the literature.[39] 10-Methyl-9,10-dihydroacridine ($AcrH_2$) was prepared according to the literature.[40] 1-(4-Substituted phenyl)-1,4-dihydronicotinamides were prepared according to the following general methods: the appropriate aniline (1 mmol) dissolved in dry methanol (15 mL) was added to a solution of 1-(2,4-dinitrophenyl)nicotinamide chloride (1 mmol) in methanol (100 mL). The resulting red solution was then heated gently overnight or until the red color faded to yellow, indicating the formation of 2,4-dinitroaniline. The solution was cooled, and the precipitated side product was removed by filtration. The filtrate was then evaporated in vacuum, and the residue was dissolved in H_2O (100 mL). The aqueous phase was then exhaustively washed with diethyl ether. The water layer was then evaporated under reduced pressure to give a crude product, which was recrystallized from methanol/diethyl ether. Reduction of the pyridinium salt was performed in aqueous basic sodium dithionite to give the appropriate reduced pyridine derivatives. *N,N,N′,N′*-tetramethyl-*p*-phenylenediamine radical cation perchlorate (TMPA$^{\bullet+}$ ClO_4^-) was obtained from the oxidation of *N,N,N′,N′*-tetramethyl-*p*-phenylenediamine by Br_2 in aqueous $NaClO_4$.[41] Reagent grade acetonitrile was distilled from P_2O_5 being passed through a column of active neutral alumina to remove water and protic impurities.

Titrated calibration experiments: The titration experiments were performed on a CSC4200 isothermal titration calorimeter in acetonitrile at 25 °C. Prior to use, the instrument was calibrated against an internal heat pulse, and the functional response was verified by determination of the heat of dilution of a concentrated sucrose solution.[42] Data points were collected every 2 s. The reaction heat was determined following 10 automatic injections from a 250 μL injection syringe (containing 2.01 mM of NADH model) into the reaction cell (1.00 mL) containing 10.87 mM *N,N,N′,N′*-tetramethyl-*p*-phenylenediamine radical cation perchlorate. Injection volumes (10 μL) were delivered at 0.5 s time intervals with 500 s between every two injections. The calibration graph is shown in Figure 2. The reaction heat was obtained by area integration of each peak except for the first.

Electrochemical experiments: All electrochemical experiments were carried out by CV (sweep rate, 100 mV s^{-1}) with a BAS-100B electrochemical apparatus in acetonitrile under an argon atmosphere as described previously.[2i] Bu_4NPF_6 (0.1M) was employed as the supporting electrolyte. A standard three-electrode assembly consisted of a glassy carbon disk as the working electronic, a platinum wire as counter electrode, and 0.1M $AgNO_3$/Ag as reference. All sample solutions were 1.0 mM. The ferrocenium/ferrocene redox couple ($Fc^{+/0}$) was taken as an internal standard. Reproducibility is generally smaller than 5 mV.

0947-6539/03/0904-0878 $ 20.00+.50/0 *Chem. Eur. J.* **2003**, *9*, No. 4

Acknowledgement

This work was supported by the National Outstanding Youth Fund (Grant No. 20125206) and the Natural Science Foundation of China (Grant Nos. 20272027 and 29972028), which are gratefully acknowledged.

[1] a) Y. Murakami, J. Kikuchi, Y. Hisaeda, O. Hayashida, *Chem. Rev.* **1996**, *96*, 721; b) M. E. Brewster, A. Simay, K. Czako, D. Winwood, H. Farag, N. Bodor, *J. Org. Chem.* **1989**, *54*, 3721; c) F. Friedlos, R. J. Knox, *Biochem. Pharmacol.* **1992**, *44*, 631.

[2] a) X.-Q. Zhu, Y. Liu, B. J. Zhao, J.-P. Cheng, *J. Org. Chem.* **2001**, *66*, 370; b) X.-Q. Zhu, H.-Y. Wang, J.-S. Wang, Y.-C. Liu, *J. Org. Chem.* **2001**, *66*, 344; c) X.-Q. Zhu, B.-J. Zhao, J.-P. Cheng, *J. Org. Chem.* **2000**, *65*, 8158; d) X.-Q. Zhu, Y.-C. Liu, J.-P. Cheng, *J. Org. Chem.* **1999**, *64*, 8980; e) X.-Q. Zhu, Y.-C. Liu, H.-Y. Wang, W. Wang, *J. Org. Chem.* **1999**, *64*, 8982; f) X.-Q. Zhu, Y.-C. Liu, *J. Org. Chem.* **1998**, *63*, 2786; g) X.-Q. Zhu, H.-L. Zou, P.-W. Yuan, L. Cao, J.-P. Cheng, *J. Chem. Soc. Perkin Trans. 2* **2000**, 1857; h) X.-Q. Zhu, Y. Liu, B.-J. Zhao, J.-P. Cheng, *J. Org. Chem.* **2001**, *66*, 370.

[3] a) T. Bally, P. Bednarek, *J. Phys. Chem. A* **2000**, *104*, 724; b) P. Bednarek, T. Bally, *J. Phys. Chem. A* **2000**, *104*, 718; c) N. Kanomata, T. Nakata, *J. Am. Chem. Soc.* **2000**, *122*, 4563; d) A. Marcinek, J. Adamus, K. Huben, J. Gbicki, T. J. Bartczak, P. Bednarek, T. Bally, *J. Am. Chem. Soc.* **2000**, *122*, 437; e) S. Fukuzumi, H. Imahori, K. Okamoto, H. Yamada, M. Fujitsuka, O. Ito, D. M. Guldi, *J. Phys. Chem. A* **2002**, *106*, 1903; f) I. Nakanishi, S. Fukuzumi, T. Konishi, K. Ohkubo, M. Fujitsuka, O. Ito, N. Miyata, *J. Phys. Chem. B* **2002**, *106*, 2372; g) H. C. Lo, C. Leiva, O. Buriez, J. B. Kerr, M. M. Olmstead, R. H. Fish, *Inorg. Chem.* **2001**, *40*, 6705; h) J. Luo, T. C. Bruice, *J. Am. Chem. Soc.* **2001**, *123*, 11952; i) S. Fukuzumi, Y. Fujii, T. Suenobu, *J. Am. Chem. Soc.* **2001**, *123*, 10191; j) B. Nidetzky, M. Klimacek, P. Mayr, *Biochem.* **2001**, *40*, 10371.

[4] a) M. F. Powell, T. C. Bruice, *J. Am. Chem. Soc.* **1982**, *104*, 5834; b) M. F. Powell, T. C. Bruice, *J. Am. Chem. Soc.* **1983**, *105*, 1014; c) J. W. Verhoeven, W. van Gerresheim, F. M. Martiens, S. M. van der Kerk, *Tetrahedron* **1986**, *42*, 975; d) L. L. Miller, J. R. Valentine, *J. Am. Chem. Soc.* **1988**, *110*, 3982; e) D. Ostovic, R. M. G. Roberts, M. M. Kreevoy, *J. Am. Chem. Soc.* **1983**, *105*, 7629.

[5] a) F. Powell, S. C. Wu, T. C. Bruice, *J. Am. Chem. Soc.* **1984**, *106*, 3850; b) B. W. Carlson, L. L. Miller, *J. Am. Chem. Soc.* **1983**, *105*, 7453; c) S. Fukuzumi, S. Koumitsu, K. Hironaka, T. Tanaka, *J. Am. Chem. Soc.* **1987**, *109*, 305; d) A. Sinha, T. C. Bruice, *J. Am. Chem. Soc.* **1984**, *106*, 7291; e) C. C. Lai, A. K. Colter, *J. Chem. Soc. Chem. Commun.* **1980**, 1115.

[6] a) L. L. Miller, J. R. Valentine, *J. Am. Chem. Soc.* **1988**, *110*, 3982, and references therein; b) B. W. Carlson, L. L. Miller, *J. Am. Chem. Soc.* **1985**, *107*, 479; c) S. Fukuzumi, S. Koumitsu, K. Hironaka, T. Tanaka, *J. Am. Chem. Soc.* **1987**, *109*, 305, and references therein; d) S. Fukuznmi, N. Nishizawa, T. Tanaka, *J. Org. Chem.* **1984**, *49*, 3571; e) C. A. Coleman, J. G. Rose, C. J. Murray, *J. Am. Chem. Soc.* **1992**, *114*, 9755.

[7] a) P. Varnai, A. Warshel, *J. Am. Chem. Soc.* **2000**, *122*, 3849; b) A. Yadav, R. M. Jackson, J. J. Holbrook, A. Warshel, *J. Am. Chem. Soc.* **1991**, *113*, 4800.

[8] a) A. Anne, P. Hapiot, J. Moiroux, P. Neta, J.-M. Saveant, *J. Am. Chem. Soc.* **1992**, *114*, 4694; b) A. Anne, S. Fraoua, V. Grass, J. Moiroux, J.-M. Saveant, *J. Am. Chem. Soc.* **1998**, *120*, 2951; c) A. Anne, S. Fraoua, J. Moiroux, J.-M. Saveant, *J. Am. Chem. Soc.* **1996**, *118*, 3938; d) P. Hapiot, J. Moiroux, J.-M. Saveant, *J. Am. Chem. Soc.* **1990**, *112*, 1337; e) A. Anne, J. Moiroux, *J. Org. Chem.* **1990**, *55*, 4608.

[9] J. Klippenstein, P. Arya, D. D. Wayner, *J. Org. Chem.* **1991**, *56*, 6736.

[10] K. L. Handoo, J.-P. Cheng, V. D. Parker, *J. Am. Chem. Soc.* **1993**, *115*, 5067.

[11] W. S. Matthews, J. E. Bares, J. E. Bartmess, F. G. Bordwell, F. J. Cornforth, G. E. Drucker, Z. Margonlin, R. J. McCallum, G. J. McCollum, N. R. Vanier, *J. Am. Chem. Soc.* **1975**, *97*, 7006.

[12] E. Arnett, K. Amarnath, N. G. Harvey, J.-P. Cheng, *J. Am. Chem. Soc.* **1990**, *112*, 344.

[13] a) D. E. Berning, B. C. Noll, D. L. DuBois, *J. Am. Chem. Soc.* **1999**, *121*, 11432; b) M. Tilset, V. D. Parker, *J. Am. Chem. Soc.* **1989**, *111*, 6711; c) G. Kiss, K. Zhang, S. L. Mukerjee, C. D. Hoff, G. C. Roper, *J. Am. Chem. Soc.* **1990**, *112*, 5657.

[14] a) T. Yao, S. Musha, M. Munemori, *Chem. Lett.* **1974**, 939; b) E. P. Platonova, V. G. Kashechko, V. Y. Atamanyuk, V. D. Pokhodenko, *Elektrokhimiya* **1980**, *16*, 674.

[15] Z.-L. Guo, Y.-C. Liu, Liu, *Chin. Sci. Bull.* **1988**, *18*, 1388.

[16] In Equations (7)–(10), free-energy change ΔG was used to replace the enthalpy change ΔH for the electron transfer processes. This treatment is reasonable because the entropies associated with electron transfer have been verified by Arnett's work (see E. M. Arnett, K. Amarnath, N. G. Harvey, J. Cheng, *J. Am. Chem. Soc.* **1990**, *112*, 344). The main reason is that the molecular structures of the products and the corresponding reactants are similar for a single electron transfer.

[17] In these estimates, irreversible redox potentials of NADH and NAD^+ models in Table 1 were used because only irreversible redox potentials of NADH and NAD^+ models are available by CV. The uncertainties were estimated generally not to be larger than 1.0 kcal mol^{-1} according to the work of Fukuzumi, in which he obtained the standard potentials of NADH model BNAH (a typical model of NADH) in acetonitrile (0.60 V) by using the fluorescence quenching method; this value is only larger than the irreversible CV peak value of BNAH (0.57 V) by 30 mV ($\approx$0.7 kcal mol^{-1}, ref: S. Fukuzumi, K. Hironaka, N. Nishizawa, T. Tanaka, *Bull. Chem. Soc. Jpn.* **1983**, *56*, 2220).

[18] J.-P. Cheng, K. L. Handoo, V. D. Parker, *J. Am. Chem. Soc.* **1993**, *115*, 2655.

[19] C. J. Curtis, A. Miedaner, W. Ellis, D. L. DuBois, *J. Am. Chem. Soc.* **2002**, *124*, 1918.

[20] a) A. van Laar, H. J. van Ramesdonk, J. W. Verhoeven, *Recl. Trav. Chim. Pays-Bas* **1983**, *102*, 157; b) W. van Gerresheim, J. W. Verhoeven, *Recl. Trav. Chim. Pays-Bas* **1983**, *102*, 339.

[21] Unlike heterolytic C–H bond scission energies, generally the BDE of the C–H bond is not very dependent on the nature of solvents.

[22] X.-M. Zhang, F. G. Bordwell, *J. Am. Chem. Soc.* **1992**, *114*, 9787.

[23] V. D. Parker, *J. Am. Chem. Soc.* **1992**, *114*, 7458.

[24] D. D. Watner, V. D. Parker, *Acc. Chem. Res.* **1993**, 26, 287.

[25] D. D. Tanner, H. K. Singh, A. Kharrat, A. R. Stein, *J. Org. Chem.* **1987**, *52*, 2142.

[26] E. S. Huyser, J. A. K. Harmony, F. L. McMillian, *J. Am. Chem. Soc.* **1972**, *94*, 3176.

[27] a) S. Fukuzumi, T. Kitano, M. Ishikawa, *J. Am. Chem. Soc.* **1990**, *112*, 5631; b) P. J. Elving in *Topics in Bioelectrochemistry and Bioenergetics*, *Vol 1* (Ed. G. Milazzo), Wiley, New York, **1976**, p. 179; c) V. Carelli, F. Liberatore, A. Casini, R. Mondelli, A. Arnone, I. Carelli, G. Retilio, I. Mavelli, *Bioorg. Chem.* **1980**, *9*, 342; d) S. Fukuzumi, T. Kitano, K. Mochida, *J. Am. Chem. Soc.* **1990**, *122*, 3246; e) X.-Q. Zhu, Y.-C. Liu, J. Li, H. Y. Wang, *J. Chem. Soc. Perkin Trans. 2* **1997**, 2191; f) E. S. Huyser, J. A. K. Harmony, F. L. McMillian, *J. Am. Chem. Soc.* **1972**, *94*, 3176.

[28] a) Y.-C. Liu, B. Li, Q. X. Guo, *Tetrahedron Lett.* **1994**, *35*, 8429; b) Y.-C. Liu, B. Li, Q. X. Guo, *Tetrahedron* **1995**, *51*, 9671; c) L. L. Miller, J. R. Valentine, *J. Am. Chem. Soc.* **1988**, *110*, 3982.

[29] S. Fukuzumi, T. Kitano, *Chem. Lett.* **1990**, 1275.

[30] B. W. Carlson, L. L. Miller, P. Neta, J. Grodkowski, *J. Am. Chem. Soc.* **1984**, *106*, 7233.

[31] A. Sinha, T. C. Bruice, *J. Am. Chem. Soc.* **1984**, *106*, 7291.

[32] According to the Hammett equation $\log K = \rho\sigma$ and $\Delta H \approx -RT \log K$, the line slope of ΔH against σ should be approximately equal to $-5.7\,\rho$.

[33] a) M. Page, A. Williams, *Organic and Bio-organic Mechanism*, Longman, **1997**, Chapter 3, pp. 52–79; b) A. Williams, *Acc. Chem. Res.* **1984**, *17*, 425; c) A. Williams, *Acc. Chem. Res.* **1989**, *22*, 387; d) A. Williams, *Adv. Phys. Org. Chem.* **1991**, *27*, 1; e) A. Williams, *J. Am. Chem. Soc.* **1985**, *107*, 6335; f) X.-Q. Zhu, Q. Li, W.-F. Hao, J.-P. Cheng, *J. Am. Chem. Soc.* **2002**, *124*, 9887.

[34] S. Fukuzumi, Y. Fujii, T. Suenobu, *J. Am. Chem. Soc.* **2001**, *123*, 10191.

[35] C4–C4 dimers of radical BNA· and its derivatives have been obtained from several experiments, which indicate that BNA· should result from the C4 radical rather than the N1 radical.

[36] a) D. F. McMillen, D. M. Golden, *Annu. Rev. Phys. Chem.* **1982**, *33*, 493; b) J. M. Dust, D. R. Arnold, *J. Am. Chem. Soc.* **1983**, *105*, 1221, and references therein.

[37] a) R. I. Walter, *J. Am. Chem. Soc.* **1966**, *88*, 1923; b) F. G. Bordwell, J.-P. Cheng, *J. Am. Chem. Soc.* **1991**, *113*, 1736, and references therein; c) J.-P. Cheng, Y. Lu, B. Liu, Y. Zhao, D. Wang, Y. Sun, J. Mi, *Sci. China Ser. B* **1998**, *41*, 215, and references therein.
[38] A. C. Anderson, G. Berkelnammer, *J. Am. Chem. Soc.* **1958**, *80*, 992.
[39] J. L. Kutz, R. Hutton, F. H. Westheimer, *J. Am. Chem. Soc.* **1961**, *83*, 584.
[40] R. M. G. Roberts, D. Ostovic, M. M. Kreevoy, *Faraday Discuss. Chem. Soc.* **1982**, *74*, 257.
[41] L. Michaelis, S. Granick, *J. Am. Chem. Soc.* **1943**, *65*, 1747.
[42] F. T. Gucker, H. B. Pickard, R. W. Planck, *J. Am. Chem. Soc.* **1939**, *61*, 459.

Received: June 17, 2002
Revised: November 7, 2002 [F4188]

  0947-6539/03/0904-0880 $ 20.00+.50/0